Available online at www.sciencedirect.com

ScienceDirect

IFAC Papers Online CONFERENCE PAPER ARCHIVE

IFAC PapersOnLine 55-20 (2022) 534–539

A linear parameter-varying modelling approach for dielectric elastomer loudspeakers ⋆

Giacomo Moretti, * **Gianluca Rizzello** *

* *Department of Systems Engineering, Saarland University, Saarbrücken, 66121 Germany (e-mails: {giacomo.moretti, gianluca.rizzello}@imsl.uni-saarland.de).*

Abstract: In this paper, we present a linear parameter-varying (LPV) model of an electrostatic loudspeaker driven by dielectric elastomer (DE) actuators. Because of its numerical simplicity, this LPV model represents a convenient tool to develop real-time control strategies for the speaker. Starting from a non-linear reduced model of the device, we assume that the control input can be broken into two components: a small-amplitude high-frequency component, responsible for the sound generation, and a slowly-varying bias component, which can be used as a free control parameter to tune and adjust the speaker response. We thus build an LPV model, treating the dynamic response to the high-frequency input component as linear, and parametrising the coefficients of such linear system with respect to the low-frequency input component. We present a validation of the model against experiments, and show that the proposed LPV formulation captures the most relevant non-linearities involved in the DE speaker operation.

Keywords: dielectric elastomer, acoustics, loudspeaker, LPV, vibro-acoustic

1. INTRODUCTION

Dielectric elastomers (DEs) are a class of multifunctional materials that exploit deformations induced by the Coulomb forces in a variable capacitor made of a deformable polymeric dielectric (see, e.g., Hajiesmaili and Clarke (2021)). Among other applications, DEs can be used to build lightweight loudspeakers, in which an electrode-covered dielectric membrane, vibrated by electrostatic forces, plays the double role of the actuator and the sound radiating surface. Because they do not make use of bulky electromagnetic actuators, DE loudspeakers are interesting candidates for the development of integrated devices for textiles and soft mechatronics. Examples of DE loudspeakers have been provided by Heydt et al. (2000); Sugimoto et al. (2013); Garnell et al. (2020).

The non-linear input-voltage vs. output-deformation relationship of DE actuators (DEAs), together with the non-linear elastic behaviour of DE membranes, renders the response of a DE loudspeaker intrinsically non-linear. In this paper, we present an alternative modeling approach for DEA loudspeakers based on the linear parameter-varying (LPV) framework (Mohammadpour and Scherer (2012)). LPV theory has already proven as an effective tool to simplify non-linear models of DEAs and, in turn, make their control system design easier (see, e.g., Rizzello et al. (2016)). Here, we extend for the first time the LPV approach to the case of DEA speakers. In this case, challenges arise due to the higher system dimensionality as well as the presence of additional acoustic dynamics.

We build upon the assumption that the driving signal fed as input into the DEA, corresponding to the square of the applied voltage, can be expressed as the sum of two components: a larger-amplitude slowly-varying bias component, and a smaller-amplitude high-frequency component. Whereas the high-frequency component is responsible for the generation of the sound pressure, the low-frequency component modifies the dynamic parameters of the system and can be used to regulate and adjust the sound intensity over time, or to concurrently generate two different outputs (linear actuation and soud generation) with a single DEA, as proposed in one of our recent works (Gratz-Kelly et al. (2022)). Building upon a physical model of the system, we propose an LPV reformulation in which the low-frequency input component is treated as the variable parameter, while control input and output are represented by the high-frequency input component and the generated acoustic pressure, respectively. We present an experimental validation of our approach, based on measurements of the acoustic pressure from a DEA speaker prototype, and a comparison between fully-non-linear (FNL) and LPV versions of the model. The LPV approach presented and validated here provides a computationally convenient tool for the analysis and real time-control of DE loudspeakers and multi-mode DEAs.

2. DYNAMIC MODEL OF A DE LOUDSPEAKER

We set our attention on a DEA system with the topology shown in Fig. 1. This device, known as cone DEA,

⋆ This project has received funding from the European Union's Horizon 2020 research and innovation programme under the Marie Skłodowska-Curie grant agreement No 893674 (DEtune). The equipment used for the tests was partly sponsored by the ME Saar Foundation through the start-up funding of Saarland University.

10.1016/j.ifacol.2022.09.150

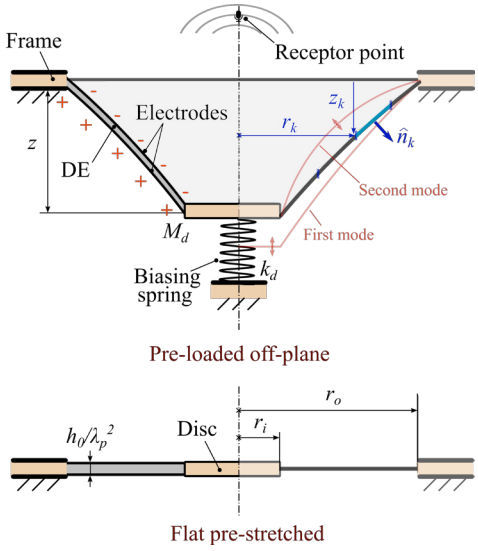

Fig. 1. Cone DEA loudspeaker: layout and model variables.

is largely used as actuator for low-frequencies (Rizzello et al. (2016)), and its application as DE loudspeaker has been studied by Sugimoto et al. (2013) and Gratz-Kelly et al. (2022), who recently proposed to use it as a multi-function interface to concurrently produce linear actuation and sound. The cone DEA consists of an electrode-covered incompressible DE membrane, with initial thickness h_0, mounted (with a certain degree of equi-biaxial pre-stretch λ_p) on a rigid annular frame (with radius r_o), holding a rigid disc (with radius r_i) at its centre. The central disc is connected to a pre-loaded mechanical spring, which causes the DE membrane to deform out-of-plane in a conical fashion. When a voltage is statically applied on the electrodes, the membrane further deforms out-of-plane, causing an axial displacement of the central disc. In our previous work (Moretti et al. (2022)), we demonstrated that this pumping motion disappears in the high frequency range, where the device follows complex deformation patterns associated with the DE membrane's structural dynamics. In loudspeakers applications, such high-frequency deformations are responsible for the generation of the acoustic pressure field.

With the aim of investigating the cone DEA's response at high-frequencies as loudspeakers, in the following we make reference to a FNL electro-elasto-acoustic model, first presented by Moretti et al. (2022), of which we present a reduced reformulation in Sect. 2.1, and we then present an LPV reformulation in Sect. 2.2.

2.1 Fully-non-linear model

The model of a cone DEA loudspeaker can be schematically represented, in a simplified manner, as a cascade of two sub-blocks (see Fig 2a): a block describing the DEA dynamics, which takes the square of the applied voltage v as input and returns the motion profiles over the membrane surface; and an acoustic block, which calculates the generated acoustic pressure p at a target point in space. We hereby make reference to a non-linear model of the cone DEA that relies on the following assumptions and simplifications: 1) statically, the DE can be modelled as an axial-symmetrical hyperelastic lossless dielectric continuum (see Dorfmann and Ogden (2014)); 2) the sound pressure field generated by the membrane vibration is related to the accelerations of the membrane points via a linear transfer function (similar to Rayleigh theory - see Quaegebeur et al. (2010)); 3) elasto-acoustic interactions (i.e., the contribution of the sound pressure p on the membrane dynamics) are accounted for in a simplified way, through a suitable choice of the dynamic parameters (i.e., no feedback coupling is present between the two sub-blocks in the model in Fig. 2a); 4) the total damping on the system can be approximately modelled as linear; 5) the continuum deformations of the membrane can be approximately represented via a finite number of degrees of freedom (Rizzello et al. (2016); Moretti et al. (2022)). Here, we parametrise the membrane's deformation kinematics via a finite superposition of mode shapes (see Fig. 1), which approximately describe the deformation patterns followed by the membrane over different frequency ranges. The equation of motion of the membrane can be expressed in the following compact form:

$$M_\alpha \ddot{\alpha} + D_\alpha \dot{\alpha} + k_\alpha(\alpha) = h_\alpha(\alpha) v^2, \tag{1}$$

where $\alpha \in \mathbb{R}^r$ is a modal coordinate (here playing the role of a lagrangian variable), which allows mapping the position of a set of points on the DE surface via a linear relationship. Denoting $q = [r_1, z_1 \ldots, r_n, z_n]^\intercal \in \mathbb{R}^{2n}$ a vector holding the radial and axial coordinates of a given combination of n target points (in general, with $n \gg r$) on the membrane surface (see, e.g., Fig. 1), α allows expressing the position of the points as follows:

$$q = q_0 + Q_\alpha \alpha, \tag{2}$$

where q_0 represents the equilibrium configuration, and $Q_\alpha \in \mathbb{R}^{2n \times r}$ is a matrix inducing a change of coordinates. The columns of Q_α represent mode shape functions, whose linear combination provides an approximated representation of q. M_α, $D_\alpha \in \mathbb{R}^{r \times r}$ are mass and damping matrices; $k_\alpha(\alpha)$ is a vector of non-linear elastic forces; $h_\alpha(\alpha)$ is an excitation coefficient. Similar to Moretti et al. (2022), we assume that M_α includes two contributions: a contribution due to the membrane mass, and a contribution due to the acoustic added mass, which is not negligible for thin lightweight membranes vibrating in air (Garnell et al. (2020)). Analogously, D_α is here assumed to account for both the DE viscous dissipation and the damping due to sound radiation. Although the acoustic added mass and damping are, in principle, complex functions of the frequency, here for simplicity we assume that M_α and D_α are diagonal and constant. This assumption is motivated by the observation (confirmed by experiments in Moretti et al. (2022)) that the each of the different mode shape functions used to parameterise the kinematics is only excited over a rather narrow frequency band, which allows neglecting the dependency of the modal added mass and damping on frequency. An explicit calculation of M_α and D_α (including the acoustic contributions) is non trivial and would demand for complex numerical approaches. Therefore, in this work, such matrices are identified using experimental data. In contrast to that, the terms rendering the DE static response ($k_\alpha(\alpha)$ and $h_\alpha(\alpha)$) are computed using a physics-based model of the DEA (Moretti et al. (2022)). The following relationships hold:

$$k_\alpha = \frac{\partial U}{\partial \alpha}, \; h_\alpha = \frac{1}{2}\frac{\partial C}{\partial \alpha}, \tag{3}$$

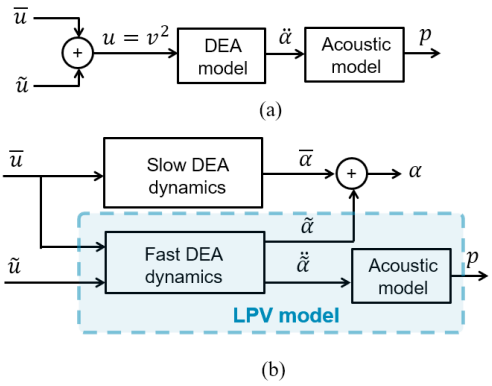

Fig. 2. Structure of the (a) FNL and (b) LPV model.

where $U(\alpha)$ is the (scalar) elastic potential energy of the system (i.e., the sum of the DE membrane hyperelastic energy and the energy of the biasing spring); and $C(\alpha)$ is the capacitance of the DE (scalar). We calculate $U(\alpha)$ and $C(\alpha)$ based on the energy-based model of cone DEAs presented in our previous works (Moretti et al. (2022), Moretti et al. (2022)). That model allows calculating the DEA capacitance and elastic energy by considering a finite set of points over the mmebrane profile and parametrising the geometry through the coordinates of such points (i.e., variable q in Eq. (2)). Detailed passages for the calculation of the cone DEA capacitance and potential energy are discussed in the reference and omitted here for conciseness. The same model (Moretti et al. (2022)) can be also used to define the mode shapes used to parametrise the kinematics (i.e., to build jacobian matrix Q_α and establish a relationship between geometrical coordinates q and modal coordinates α). This is done by calculating the uncoupled eigenmodes of the undamped DEA (i.e., neglecting the acoustic added mass and all damping contributions, and using linearised analytical expressions for the DEA stiffness and inertia, as given by Moretti et al. (2022)) and using them to infer the coordinate change in (2). Although the mode shapes identified with this procedure do not represent the eigenmodes of system (1) (i.e., coordinate change (2) does not represent an exact modal transcription of the dynamics), they still provide an effective parametrisation of the DEA kinematics. In fact, the contributions of acoustic coupling terms and damping in (1) are not expected to significantly affect the shape of the DEA's eigenmodes compared to the undamped uncoupled scenario (as observed in Moretti et al. (2022)), but just their eigenfrequencies. We also remark that the parametrisation of the kinematics used here has the advantage of 1) reducing the model dimension, compared to using the coordinates of a set of target points on the DE as the coordinates; 2) describing the dynamics by means of shape functions that are close to the system eigenfrequencies (which allows calibrating the unknown parameters, M_α, D_α, based on the measured modal response of the system, as explained in Sect. 3.2).

For simplicity, we further assume that the acoustic pressure output is related linearly (i.e., through a linear transfer function) to the accelerations of the points on the membrane surface, as stated by Rayleigh theory (see Quaegebeur et al. (2010)). Analytical expressions to put the acoustic pressure p at receptor point in relation to the acceleration of the radiating surface can only be obtained for simple geometries (i.e., pulsating spheres or rigid pistons). For convenience, in this work, we assume that the sound pressure at the receptor point is expressed by means of a linear state-space model, whose parameters are identified based on experimental data (see Sect. 3):

$$\begin{cases} \dot{\xi} = F\xi + G\ddot{\alpha} \\ p = H\xi \end{cases}, \tag{4}$$

where ξ represents a state vector describing the acoustic response, and F, G, H are suitably identified matrices.

The combination of (1) and (4) is hereby denoted as the FNL DE loudspeaker model, as opposed to the LPV formulation discussed in the following.

2.2 LPV model

With the aim of developing the LPV reformulation, the following assumptions are introduced:

Assumption 1. The control input of the DE loudspeaker is given as the sum of two terms:

$$v^2(t) := u(t) = \bar{u}(t) + \tilde{u}(t),\ |\tilde{u}(t)| \ll |\bar{u}(t)|\ \forall\ t. \tag{5}$$

Term $\bar{u}$ represents a slowly-varying, large-amplitude bias, which can be adjusted over time to tune and regulate the speaker response. Term $\tilde{u}$ represents the high-frequency, low amplitude acoustic input responsible for the sound pressure generation.

Assumption 2. Upon application of input (5), the membrane deformation can be expressed as the sum of two components, namely:

$$\alpha(t) = \bar{\alpha}(t) + \tilde{\alpha}(t),\ |\tilde{\alpha}(t)| \ll |\bar{\alpha}(t)|\ \forall\ t. \tag{6}$$

Here, $\bar{\alpha}$ is the solution to (1) obtained for $v^2 = \bar{u}$, namely

$$M_\alpha\ddot{\bar{\alpha}} + D_\alpha\dot{\bar{\alpha}} + k_\alpha(\bar{\alpha}) = h_\alpha(\bar{\alpha})\bar{u}, \tag{7}$$

while $\tilde{\alpha}$ is a residual term appearing in case (1) is driven by $v^2 = \bar{u} + \tilde{u}$; $\bar{\alpha}$ is expected to be much slower than $\tilde{\alpha}$.

Assumption 3. Term $\bar{u}$ varies on a significantly slower time-scale than any of the eigenfrequencies of the system. Therefore, on the time-scale of $\tilde{\alpha}$, deformation component $\bar{\alpha}$ can be considered as practically stationary, and can be tightly approximated with the static response of the system to $\bar{u}$:

$$\bar{\alpha} \simeq \bar{\alpha}_s(\bar{u}),\ \text{with}\ k_\alpha(\bar{\alpha}_s) - h_\alpha(\bar{\alpha}_s)\bar{u} = 0. \tag{8}$$

Assumption 4. The acoustics pressure p, as given by (4), only depends on the high-frequency component $\tilde{\alpha}$, as $\bar{\alpha}$ is slower than any acoustically relevant dynamics.

The choice of an excitation input as in (5) (Assumption 1) has been recently proved to enable the employment of cone DEAs as multi-function interfaces, capable of concurrently producing a linear actuation and sound (Gratz-Kelly et al. (2022)). Note that, since (1) is a nonlinear system, the superposition principle does not hold, thus $\tilde{\alpha}$ formally depends on both $\bar{u}$ and $\tilde{u}$. Nevertheless, due to the characteristics of signals $\bar{u}$ and $\tilde{u}$, it is reasonable to assume that Assumptions 2-4 hold true as well.
Linearising (1) around trajectory $\bar{\alpha}$ as given by (7), and considering Assumptions 1-3, we obtain the following:

$$\begin{aligned} &M_\alpha\ddot{\tilde{\alpha}} + D_\alpha\dot{\tilde{\alpha}} + S_\alpha(\bar{\alpha}_s(\bar{u}))\tilde{\alpha} = h_\alpha(\bar{\alpha}_s(\bar{u}))\tilde{u}\ \text{, with} \\ &S_\alpha(\alpha) = \frac{\partial k_\alpha(\alpha)}{\partial\alpha} - \bar{u}\frac{\partial h_\alpha(\alpha)}{\partial\alpha} \end{aligned} \tag{9}$$

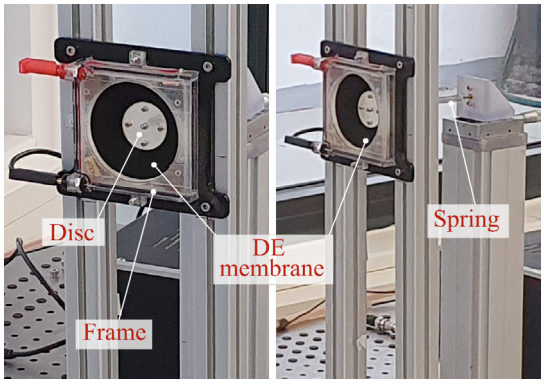

Fig. 3. Pictures of the cone DEA speaker prototype.

We define $x = \left[\dot{\bar{\alpha}}^\intercal \ \tilde{\alpha}^\intercal \ \xi^\intercal\right]^\intercal$ and, thanks to Assumption 4, we rewrite (9) and (4) in a compact LPV form as follows:

$$\begin{cases} \dot{x} = A_s(\bar{u})x + B_s(\bar{u})\tilde{u} \\ p = C_s x \end{cases}, \text{with}$$

$$A_s(\bar{u}) = \begin{bmatrix} -M_\alpha^{-1}D_\alpha & -M_\alpha^{-1}S_\alpha(\bar{\alpha}_s(\bar{u})) & 0 \\ I & 0 & 0 \\ -GM_\alpha^{-1}D_\alpha & -GM_\alpha^{-1}S_\alpha(\bar{\alpha}_s(\bar{u})) & F \end{bmatrix} \quad (10)$$

$$B_s(\bar{u}) = \begin{bmatrix} M_\alpha^{-1}h_\alpha(\bar{\alpha}_s(\bar{u})) \\ 0 \\ GM_\alpha^{-1}h_\alpha(\bar{\alpha}_s(\bar{u})) \end{bmatrix}, \ C_s = [0\ 0\ H].$$

where I is an identity matrix of appropriate dimension, and $\bar{u}$ plays the role of the varying parameter.

Combining (7) (dynamics of $\bar{\alpha}$) and (10) (dynamics of $\tilde{\alpha}$), the DE speaker model can be recast as the combination of a slow dynamics for $\bar{\alpha}$ and a faster dynamics for $\tilde{\alpha}$ (see Fig 2b). For the aim of the output pressure calculation, only the LPV part of the model is relevant, whereas slow dynamics (7) are only relevant to the calculation of the total membrane deformation α (see (6)). Compared to the FNL model (1), the proposed LPV formulation is computationally more convenient, and features a structure which allows for control-oriented model inversion.

3. VALIDATION AND DISCUSSION

3.1 Experimental setup and measurements

We developed a and characterised a prototype of a cone DEA (see Fig. 3), similar to that presented by Moretti et al. (2022). The device consists of a 100-μm thick DE membrane (silicone Elastosil 2030), covered by carbon-loaded screen-printed silicone electrodes (Fasolt et al. (2017)). The features of the system are summarised in Tab. 1. The DEA prototype was electrically driven with a high-voltage amplifier Trek 609E-6. The prototype was mounted in a vertical position by means of a rigid frame (see Fig. 3). A microphone (MM210 by Microtech Gefell) was located in front of the prototype, at a distance of 300 mm from the holding frame, aligned with the cone DEA axis. Measurements of the velocity/displacement at target points over the DEA were performed using a 3D Doppler laser vibrometer PSV-500 3D by Polytec.

For the aim of exemplification and validation, we considered the system response in a restricted frequency range. With the aim of identifying the natural frequencies and

Table 1. Reference DEA parameters

DE material	Silicone Elastosil 2030
Inner and outer radii	$r_i = 17$ mm, $r_o = 35.5$ mm
Unstretch. membr. thickness	$h_0 = 100$ μm
Pre-stretch	$\lambda_p = 1.2$
Elastic shear modulus (undeform.)	$\mu = 600$ kPa
Relat. dielect. permittivity	$\varepsilon_r = 2.8$
Initial out-of-plane displ.	$z = 15$ mm
Disc mass	$M_d = 5.3$ g
Spring stiffness	$k_d = 52$ N/m
Membrane mass	$M_m = 0.3$ g

deformation modes of the DEA, we measured the distribution of the velocity over the DEA surface through the 3D vibrometer, similar to Moretti et al. (2022). We performed velocity measurements at 80 points equally distributed points along 16 equally-spaced radii over the DE's electrode surface, and 4 points on the DEA central disc. We used a periodic chirp with constant bias of 2 kV and amplitude of 100 V as the voltage input. Fig. 4 shows the resulting spectra for the axial and radial velocity components. In the plots, average spectra (averaged over all points) are considered, which represent standard metrics (directly computed by the vibrometer proprietary software) that provide a general understanding of the membrane modal behaviour (see also Nalbach et al. (2019)). The peaks in the spectra correspond to system's resonances. There are two main peaks within the considered range. The first peak (corresponding to a natural frequency of approximately 55 Hz) is only present in the axial velocity spectrum, and it is associated with the pistonic out-of-plane motion of the DEA (i.e., axial motion of the central disc), hereafter called the pumping mode. The second peak (at 395 Hz) is characterised by transversal motions of the membrane (both in the radial and axial direction), which reach maximum amplitude close to the membrane average circumference (see Fig. 1). Because the mass of the central disc is much larger than the membrane's mass (see Tab. 1), the central disc motion is negligible at this frequency. This second mode is hereby called a structural mode. Since the pumping mode's pass-band lies low in the frequency range, the acoustic response is mainly governed by the structural mode (see also Moretti et al. (2022)). Other peaks with much smaller amplitude are also visible in the spectra. These are either due to dynamic contributions from the biasing spring, or non-axial-symmetrical structural modes of the membrane, and they are neglected in our model, as they play a minor role in the average spectral velocity and acoustic response (see Moretti et al. (2022)), and they are only excited as a result of inhomogenieites and asymmetries in the system, which are difficult to model.

3.2 Model validation

In the following, comparisons between experiments, FNL model (1), and LPV model (10) results are presented, with the aim of validating the presented model and estimating the accuracy of the LPV reduction. The dynamic model (FNL and LPV versions) was implemented in Matlab and Simulink. Calculation of the mode shape functions used to describe the kinematics (see (2)), $K(\alpha)$ and $h(\alpha)$ were performed using the approach presented by Moretti et al.

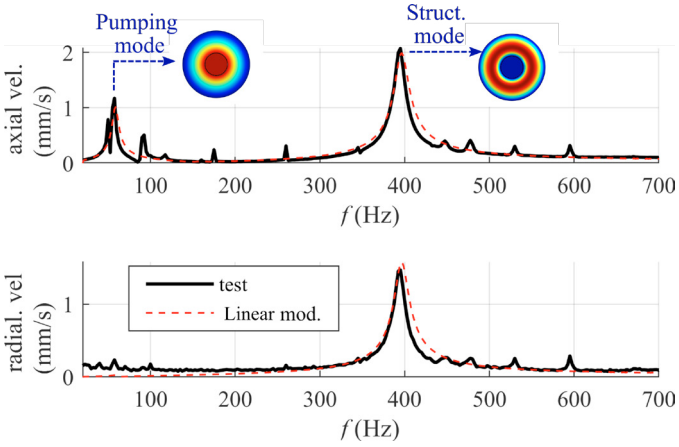

Fig. 4. Average spectra of the axial and radial velocity over the DEA membrane surface.

(2022), using a discretisation of the membrane into 7 rings. M_α and D_α have been calibrated using the spectral results of Fig. 4. Their elements (diagonal) are calculated in such a way that the peaks in the spectrum match the experimental data (both in terms of frequency abscissa and magnitude). For the aim of calibration and comparison with the spectral measurements in Fig. 4, a linearised version of the model was used, since in this test the excitation amplitude is much smaller than the (constant) bias, and the FNL and LPV versions of the model are practically equivalent.

To validate the model, we used voltage waveforms in the same form as (5), where $\bar{u}$ and $\tilde{u}$ represent periodic waveforms with fundamental frequency of f_l and f_h respectively. The time-series of the input u (i.e., the square of the applied votlage v), the central disc displacement z, and the time-varying sound pressure level (SPL) produced by the DEA (experiments vs. model) are shown in Fig. 5, for different tests. The SPL is defined as follows:

$$SPL = 20 \log_{10} \left(\frac{p_{rms}}{p_0} \right), \tag{11}$$

where $p_0 = 20$ μPa is a reference pressure, and p_{rms} is the root-mean-square value of p calculated on a moving window with length of 20 ms (i.e., mach larger than the high-frequency signal period). In the different tests, the slow component $\bar{u}$ has bias of 5 kV^2 and amplitude of 4 kV^2, whereas its frequency and waveform were changed throughout the different tests. A fundamental frequency $f_h = 390$ Hz (close to the resonance frequency of the structural mode - see Fig. 4) was used for $\tilde{u}$. The amplitude of $\tilde{u}$ is constant and equal to 0.4 kV^2 in Figs. 5a-c, whereas a time-varying amplitude is used in Fig. 5d. The acoustic model matrices (F, G, H in (4)) have been identified via Matlab command *ssest* based on the dataset in Fig. 5c, using $\ddot{\alpha}$ from the FNL model simulations as the input, and the experimentally measured pressure as the output. A second-order model (namely, $\xi \in \mathbb{R}^2$) was used for the identification.

Using constant-amplitude sinusoidal waveforms for $\bar{u}$ and $\tilde{u}$ (Fig. 5a) results in a SPL whose amplitude is not constant over time. In particular, the sound level is maximum (minimum) when the low frequency component $\bar{u}$ has maximum (minimum) amplitude. This is a non-linear effect due to a variation in the DE stiffness induced by the applied voltage. Increasing the applied voltage causes a decrease in the stress on the DE membrane (due to electrostatic stress contributions) and, hence, larger amplitude vibrations in response to the high-frequency stimulus $\tilde{u}$, which result in larger values of p. This effect is correctly captured by both the FNL and the LPV implementations of the model. Similar trends are also observed by considering a higher value of f_l (Fig. 5b), or a different waveform for $\bar{u}$ (Fig. 5c). In particular, using a square wave, the trend of the SPL sensibly changes compared to using sinusoidal $\bar{u}$ (compare Figs. 5a and 5c). Whereas the SPL trend in Fig. 5a closely follows the profile of $\bar{u}$, the SPL in Fig. 5c has a smoother profile than $\bar{u}$, as a result of the system low-pass dynamics.

In Fig. 5d, $\tilde{u}$ is recast as a sine waveform with modulated amplitude. In particular, the amplitude of $\tilde{u}$ varies linearly following the same trend as $\bar{u}$, it is minimum (and equal to 0.4 kV^2) when $\bar{u}$ is maximum, and it is maximum (equal to 0.7 kV^2) when $\bar{u}$ is minimum. By doing so leads to a more uniform amplitude of the acoustic output (as compared to Fig. 5a), as the amplitude of the acoustically relevant input, $\tilde{u}$, is larger in the phases in which the DE is stiffer. The model consistently predicts the reduction in the SPL fluctuation obtained by using an amplitude modulation for the high-frequency input (Fig. 5d).

The axial displacement of the central disc is only affected by $\bar{u}$, i.e., the dynamics of the central disc filters out the higher frequency contribution of $\tilde{u}$, because of the small passband of the pumping mode. Whereas z in Figs. 5a, b, d simply follows the trend of $\bar{u}$, higher-frequency vibrations are present in Fig. 5c. These are free oscillations at the natural frequency of the pumping mode, and are triggered by jumps in the input. The LPV model produces results that are in close agreement with the FNL model, and it is able to capture the main features of the system dynamics response, including non linear effects triggered by the DEA's stiffness variations. A quantitative evaluation of the LPV model accuracy (in terms of the estimated axial position z and the SPL) is presented in Tab. 2. The error is computed as follows:

$$\text{err.} = \frac{||\phi_{\text{LPV}} - \phi_{\text{ref}}||}{||\phi_{\text{ref}}||}, \tag{12}$$

where ϕ represents a generic signal (here, z or the SPL) obtained through the LPV model (subscript SPL) as opposed to the same signal obtained in a reference scenario (test or FNL model - subscript ref), and $||.||$ is the $\mathcal{L}_2$-norm. The differences between the LPV and the FNL model are always below 0.5%, and the maximum error with respect to the experiments is below 2%.

In conclusion, we proved that an LPV model is able to accurately describe the dynamics of a cone DEA loudspeaker. By building upon an assumption of the deformation kinematics, the model allows determining the acoustic response of the DEA when multiple modes are excited at

Table 2. Model accuracy evaluation

Test (Fig. 5)	**Error LPV-FNL**		**Error LPV-exp.**	
	z	SPL	z	SPL
(a)	$< 0.1\%$	0.2%	0.2%	1.0%
(b)	$< 0.1\%$	0.5%	0.3%	1.5%
(c)	$< 0.1\%$	0.5%	0.3%	0.8%
(d)	0.1%	0.6%	0.5%	1.5%

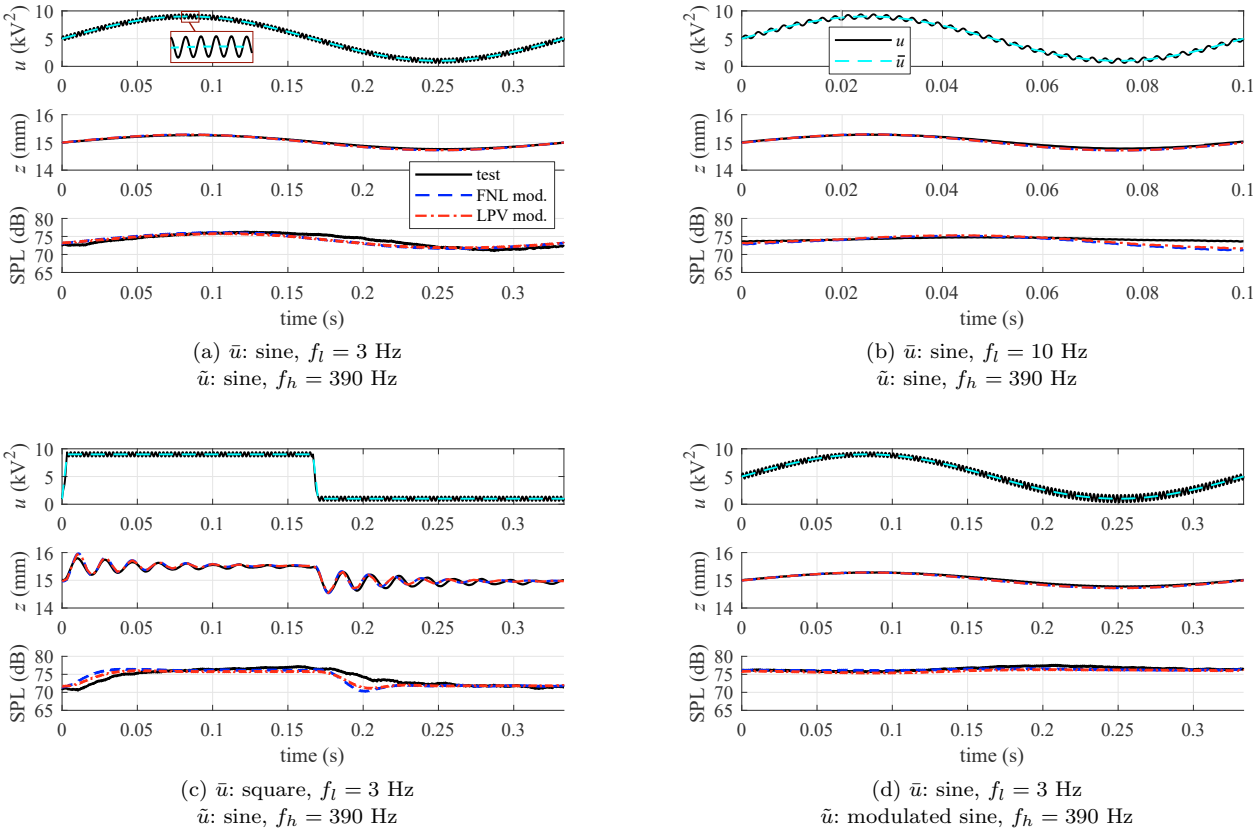

(a) $\bar{u}$: sine, $f_l = 3$ Hz
$\tilde{u}$: sine, $f_h = 390$ Hz

(b) $\bar{u}$: sine, $f_l = 10$ Hz
$\tilde{u}$: sine, $f_h = 390$ Hz

(c) $\bar{u}$: square, $f_l = 3$ Hz
$\tilde{u}$: sine, $f_h = 390$ Hz

(d) $\bar{u}$: sine, $f_l = 3$ Hz
$\tilde{u}$: modulated sine, $f_h = 390$ Hz

Fig. 5. Time-series of input u (i.e., the squared applied voltage $u = v^2$), central disc displacement z, and SPL for different tests with different inputs. The lines in the top sub-plots represent u (total excitation signal) and $\bar{u}$ (low-frequency trend). The different lines in the other sub-plots refer to the tests, the FNL and the LPV model.

the same time. Moreover, the model consistently captures the non-linear effect (namely, modulation of the SPL) of slowly varying the applied bias voltage, while preserving a simple and computationally-convenient structure. In the future, we will employ this LPV approach to investigate advanced control strategies for multi-mode DEAs, with the aim of exploring their combined application as linear actuators and loudspeakers (Gratz-Kelly et al. (2022)).

REFERENCES

Dorfmann, L. and Ogden, R.W. (2014). *Nonlinear theory of electroelastic and magnetoelastic interactions*. Springer.

Fasolt, B., Hodgins, M., Rizzello, G., and Seelecke, S. (2017). Effect of screen printing parameters on sensor and actuator performance of dielectric elastomer (DE) membranes. *Sensors and Actuators A: Physical*, 265, 10–19.

Garnell, E., Doaré, O., and Rouby, C. (2020). Coupled vibro-acoustic modeling of a dielectric elastomer loudspeaker. *The Journal of the Acoustical Society of America*, 147(3), 1812–1821.

Gratz-Kelly, S., Rizzello, G., Fontana, M., Seelecke, S., and Moretti, G. (2022). A multi-mode, multi-frequency dielectric elastomer actuator. *Advanced Functional Materials*, in print.

Hajiesmaili, E. and Clarke, D.R. (2021). Dielectric elastomer actuators. *Journal of Applied Physics*, 129(15), 151102.

Heydt, R., Pelrine, R., Joseph, J., Eckerle, J., and Kornbluh, R. (2000). Acoustical performance of an electrostrictive polymer film loudspeaker. *The Journal of the Acoustical Society of America*, 107(2), 833–839.

Mohammadpour, J. and Scherer, C.W. (2012). *Control of linear parameter varying systems with applications*. Springer Science & Business Media.

Moretti, G., Rizzello, G., Fontana, M., and Seelecke, S. (2022). Modelling and experimental characterization of voltage-driven vibrations in dielectric elastomer membranes. *Mechanical Systems and Signal Processing*, 168.

Nalbach, S., Rizzello, G., and Seelecke, S. (2019). Experimental analysis of continuous vibrations in dielectric elastomer membrane actuators via three-dimensional laser vibrometry. *Journal of Vibration and Acoustics*, 141(5).

Quaegebeur, N., Chaigne, A., and Lemarquand, G. (2010). Transient modal radiation of axisymmetric sources: Application to loudspeakers. *Applied Acoustics*, 71(4), 335–350.

Rizzello, G., Naso, D., Turchiano, B., and Seelecke, S. (2016). Robust position control of dielectric elastomer actuators based on lmi optimization. *IEEE Transactions on Control Systems Technology*, 24(6), 1909–1921.

Sugimoto, T., Ando, A., Ono, K., Morita, Y., Hosoda, K., Ishii, D., and Nakamura, K. (2013). A lightweight push-pull acoustic transducer composed of a pair of dielectric elastomer films. *The Journal of the Acoustical Society of America*, 134(5), EL432–EL437.